

# Skin Delivery of siRNA Using Sponge Spicules in Combination with Cationic Flexible Liposomes

XueJiao Liang,<sup>1</sup> JiaLiang Zhang,<sup>2</sup> HuiLong Ou,<sup>1</sup> Jun Chen,<sup>1</sup> Samir Mitragotri,<sup>3</sup> and Ming Chen<sup>1,4</sup>

<sup>1</sup>State-Province Joint Engineering Laboratory of Marine Bioproducts and Technology, Department of Marine Biological Science & Technology, College of Ocean and Earth Sciences, Xiamen University, Xiamen 361102, China; <sup>2</sup>Department of Pharmacy, Dong Fang Hospital (Fuzhou General Hospital), Medical College of Xiamen University, Xiamen University, Fuzhou 350025, China; <sup>3</sup>School of Engineering and Applied Sciences, Harvard University, Cambridge, MA 02138, USA; <sup>4</sup>State Key Laboratory of Marine Environmental Science, College of Ocean & Earth Sciences, Xiamen University, Xiamen 361102, China

**We report the topical administration of sponge *Haliclona* sp. Spicules (SHS) combined with cationic flexible liposomes (CFL) to increase the delivery of small interfering RNA (siRNA) into viable skin cells *in vitro* and *in vivo*. SHS can be applied topically as novel microneedles to overcome skin barrier by creating plenty of new microchannels in stratum corneum. Subsequently, well-designed CFL can be also utilized topically as nanocarriers to overcome skin cells membrane by delivering siRNA to skin deep layers through these microchannels and thereby facilitating their cell internalization. The topical application of SHS in combination with CFL (0.05% of lipids, w/v), referred to as CFL(0.05%), enhanced siRNA skin penetration *in vitro* by  $72.95 \pm 2.97$ -fold compared to control group ( $p < 0.001$ ). Further, the topical application of SHS in combination with CFL(0.05%) on female BALB/c mice skin resulted in  $29.21\% \pm 1.41\%$  of glyceraldehyde-3-phosphate dehydrogenase (GAPDH) knockdown at all application area *in vivo*, which was not significantly different from the GAPDH protein knockdown rate in the subcutaneous injection center. However, the high knockdown rate only appears in the vicinity ( $<0.5$  cm) of the injection center. In sum, this study provides a promising strategy of topical delivery of siRNA by the combined used of SHS and well-designed CFL.**

## INTRODUCTION

RNA interference (RNAi) is to inhibit gene expression sequence, specifically using short double-stranded RNA (21 to 23 nucleotides, small interfering RNA [siRNA]).<sup>1,2</sup> RNAi therapy so far has been proven to have great potential to treat skin diseases stem from aberrant gene expression,<sup>3</sup> including alopecia,<sup>4</sup> psoriasis,<sup>5</sup> allergic skin diseases,<sup>6,7</sup> skin cancer,<sup>5,8,9</sup> pachyonychia congenita,<sup>10</sup> and hyperpigmentation,<sup>11</sup> among others. For the specific gene suppression in these skin diseased regions, topical application of RNAi therapy can avoid first pass metabolism and side-effect involved by systemic administration. It also can exert its action directly on the skin diseased site and improve patient compliance, and so on.<sup>12,13</sup>

Since siRNA is a hydrophilic and negatively charged bio-macromolecule (~13 kDa), its topical delivery into viable skin cells generally meets two barriers. The first barrier of the delivery is the stratum corneum

(SC) because of the “brick and mortar” construction and lipophilic nature.<sup>14,15</sup> To overcome this skin barrier, various penetration enhancement strategies and technologies have been developed and utilized, such as microneedle,<sup>16,17</sup> chemical penetration enhancers,<sup>18</sup> and nanocarrier systems,<sup>19,20</sup> among others. The second barrier of the topical delivery of siRNA is the viable skin cells membrane.<sup>21</sup> To overcome this challenge, we utilized a number of methods to facilitate internalization of siRNA, such as electroporation,<sup>22</sup> lipoplex,<sup>23,24</sup> and heat-shock,<sup>25</sup> among others.<sup>18,26–31</sup> However, physical delivery techniques, such as microneedle patch,<sup>32</sup> sonophoresis,<sup>33</sup> iontophoresis,<sup>34</sup> electroporation,<sup>35</sup> and heat-shock, despite their relatively high efficacy to overcome skin barrier or cytoplasm barrier of viable cells, can be applied only to small areas of the skin and have limited potential for self-administration. In addition, some of these methods are invasive. On the other hand, chemical delivery techniques, such as nanocarriers and penetration enhancers, are ineffective to be utilized alone to overcome the both barriers to deliver siRNA into skin viable cells.<sup>36</sup> In addition, the long-term usage of chemical penetration enhancers can lead to skin irritation because of their cytotoxicity.<sup>37</sup> Therefore, there could be a lurking but reasonable expectation that a certain topical delivery system can be well designed and fabricated not only to overcome both skin barrier and cytoplasm barrier for the delivery of siRNA into skin viable cells, but also to be adapted to any location of interest or diseased area of the skin with a non-invasive or a minimally invasive way.

Recently, we have shown that sponge *Haliclona* sp. spicules (SHS), as novel silicon microneedles, can be used alone<sup>38</sup> or in combination with flexible liposomes<sup>39</sup> to overcome skin barrier for enhanced skin absorption of hydrophilic macromolecules. SHS can create plenty of new long-lasting micro-channels (around 800 micro-pores per mm<sup>2</sup> over 48 h at a dosage of 10 mg of SHS per 1.77 cm<sup>2</sup>) through or into the SC in a minimally invasive way.<sup>39</sup> However, even with using SHS, the cytoplasm barrier is still a big challenge for the topical delivery of siRNA into skin viable cells.

Received 18 February 2020; accepted 13 April 2020;  
<https://doi.org/10.1016/j.omtn.2020.04.003>

**Correspondence:** Ming Chen, State Key Laboratory of Marine Environmental Science, College of Ocean & Earth Sciences, Xiamen University, Xiamen 361102, China.

**E-mail:** [ming.chen@xmu.edu.cn](mailto:ming.chen@xmu.edu.cn)



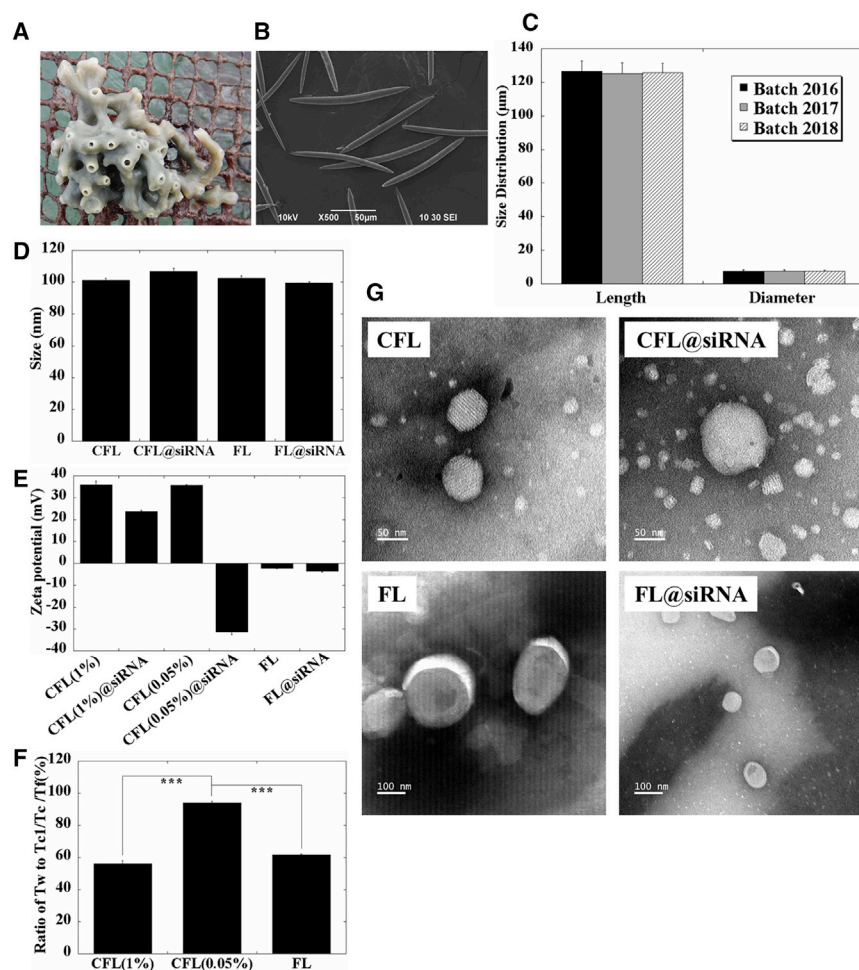


**Figure 1. Characterization of SHS and Lipid Vesicles**

(A) Photo of Sponge *Haliclona* sp. (B) Visualization of SHS by SEM. (C) Statistics of SHS size in different batches. (D) Mean particle diameter of lipid vesicles. (E)  $\zeta$ -potential of lipid vesicles. (F) Deformability of lipid vesicles. (G) Visualization of lipid vesicles by TEM. Values represent mean  $\pm$  SD ( $n = 100$  for C;  $n = 3$  for D–F)

positive  $\zeta$ -potential of  $35.7 \pm 0.4$  mV. When mixed with siRNA, CFL(0.05%)@siRNA exhibited a similar particle size distribution and PDI, however possessed a negative  $\zeta$ -potential of  $-31.4 \pm 1.1$  mV. Flexible liposomes without or with siRNA (FL or FL@siRNA, Figure 1G) were both homogeneously nano-sized unilamellar spherical vesicles (mean diameter of around 102.5 nm with a PDI of around 0.08) with a neutral  $\zeta$ -potential of about  $-2.2$  mV. Optimized CFL (0.05%) possessed a better deformability ( $94.08 \pm 1.01\%$ ,  $p < 0.001$ ) compared to original CFL (1%,  $56.03 \pm 1.98\%$ ) and FL (4%,  $61.79 \pm 0.48\%$ ).

#### Improved Topical Delivery of siRNA *In Vitro*

To overcome the first barrier of siRNA topical delivery, we topically applied SHS alone or in combination with different lipid vesicles containing GAPDH-siRNA. The topical application of SHS combined with CFL(0.05%) could significantly improve the skin penetration of siRNA compared to all other groups (Figure 2); it led to skin absorption of  $61.18 \pm 2.49\%$  of topically applied GAPDH-siRNA in 16 h, which is  $72.95 \pm 2.97$ -fold ( $p < 0.001$ ),  $14.77 \pm 0.60$ -fold ( $p < 0.001$ ),  $11.45 \pm 0.47$ -fold ( $p < 0.001$ ),  $1.88 \pm 0.08$ -fold ( $p < 0.01$ ), and  $1.61 \pm 0.07$ -fold ( $p < 0.001$ ) higher than those of control group ( $0.84 \pm 0.16\%$ ), CFL(0.05%) alone ( $4.14 \pm 0.73\%$ ), Dermal roller combined with CFL(0.05%) ( $5.34 \pm 0.72\%$ ), SHS alone ( $32.55 \pm 8.90\%$ ), and SHS combined with FL ( $37.99 \pm 1.52\%$ ), respectively. The skin absorption of siRNA from the topical application of SHS combined with CFL(0.05%) is significantly higher than that from the topical application of SHS combined with CFL(1%) ( $48.19 \pm 7.21\%$ ,  $p < 0.05$ ). The result indicated that the capability of CFL to deliver siRNA into skin after SHS treatment seems to be proportional to its deformability.

Moreover, the topical application of SHS combined with CFL (0.05%) could significantly increase the skin deposition of siRNA compared to other groups (Figure 3). In addition, the skin penetration behavior of siRNA from different topical formulation *in vitro* was visualized by confocal microscopy (Figure 4). These results confirmed that the topical application of SHS combined CFL (0.05%) could significantly enhance the delivery of siRNA into skin (Figure 4H) compared to all other groups.

In this work, we topically applied SHS in combination with different lipid vesicles, flexible liposomes (FL) and cationic flexible liposomes (CFL), to greatly enhance skin penetration of siRNA *in vitro*. Further, the combined use of SHS and CFL(0.05%) can result in a synergistic action to deliver siRNA to viable skin cells and consequently significantly inhibit the protein expression *in vivo*, which is comparable to the subcutaneous injection of CFL(0.05%)@siRNA mixture. In addition, the combined topical use of SHS and well-designed CFL can be adapted to any location of interest or diseased area of the skin.

## RESULTS

### Characterization of SHS and Lipid Vesicles

SHS from sponge *Haliclona* sp. cultured in 2018 exhibited similar length (around 125  $\mu\text{m}$ ) and diameter (around 7.5  $\mu\text{m}$ ) distribution as that of previous batches (Figure 1C) (batch16 versus batch17:  $p = 0.626$ , batch16 versus batch18:  $p = 0.411$ , batch17 versus batch18:  $p = 0.780$ ). Cationic flexible liposomes (CFL, Figure 1G) were homogeneously nano-sized unilamellar spherical vesicles (mean diameter of  $101.4 \pm 1.1$  nm, polydispersity index (PDI) of  $0.14 \pm 0.04$ ) with a

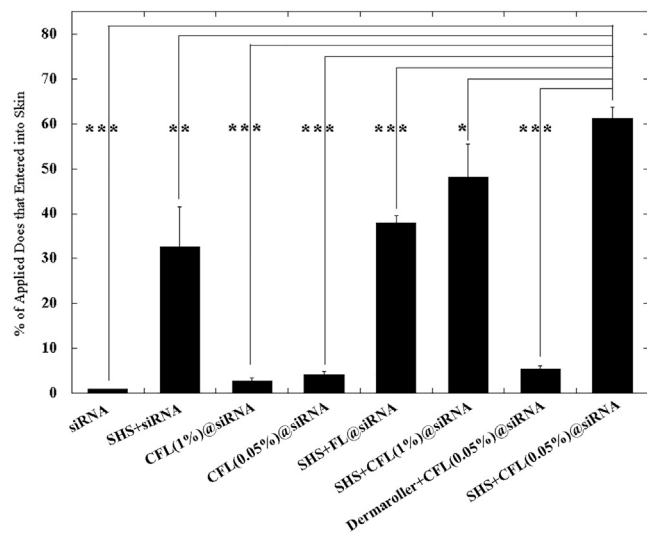


**Figure 2. Total Amount of GAPDH-siRNA Entering Skin under Different Topical Treatments**

Values represent mean  $\pm$  SD (n = 3). \*p < 0.05; \*\*p < 0.01; \*\*\*p < 0.001.

### siRNA Entry into Cells and Knockdown of GAPDH *In Vitro*

To overcome the second barrier, viable skin cells cytoplasm, we next evaluated the capabilities of three lipid vesicles, CFL(0.05%), CFL(1%), and FL, to facilitate the internalization of 6-carboxy-fluorescein (FAM)-GAPDH siRNA in L929 cell by using confocal microscopy (Figure 5). CFL (0.05%) can induce obvious cell entry of fluorescent FAM-siRNA (Figure 5) compared to other groups. In contrast, siRNA alone cannot enter the cells by itself.

Further, we also examined the GAPDH protein knockdown in L929 cell lines to verify the cell transfection effect (Figure 6). CFL(0.05%)@siRNA can result in  $41.09\% \pm 5.14\%$  of GAPDH knockdown in 68 h, which was much higher ( $p < 0.001$ ) than that from CFL(1%)@siRNA ( $8.38\% \pm 2.08\%$ ), FL@siRNA ( $3.48\% \pm 2.25\%$ ), and siRNA alone ( $6.07\% \pm 1.62\%$ ).

### Cytotoxicity of Lipid Vesicles

The cytotoxicity of CFL(0.05%), CFL(1%), and FL was studied as a function of applied dose by using thiazolyl blue tetrazolium bromide (MTT) assay. The results (Figure 7A) indicated that  $IC_{50}$  values of CFL(0.05%), CFL(1%), and FL for cell growth were  $6.634 \mu\text{L/well}$ ,  $0.626 \mu\text{L/well}$ , and  $0.428 \mu\text{L/well}$ , respectively. As the dose of the added lipid vesicles was reduced, the cell state gradually recovered (Figure 7B). These results indicated that CFL(0.05%) with appropriate dose is more suitable for delivering siRNA into cells without cytotoxicity.

### *In Vivo* Verification of GAPDH siRNA Delivery into Skin

According to skin penetration study *in vitro*, cell transfection *in vitro*, and cytotoxicity *in vitro*, the topical application of SHS combined with CFL(0.05%) seems to be the most effective system for topical application of RNAi. Thus, we subsequently verified the ability of

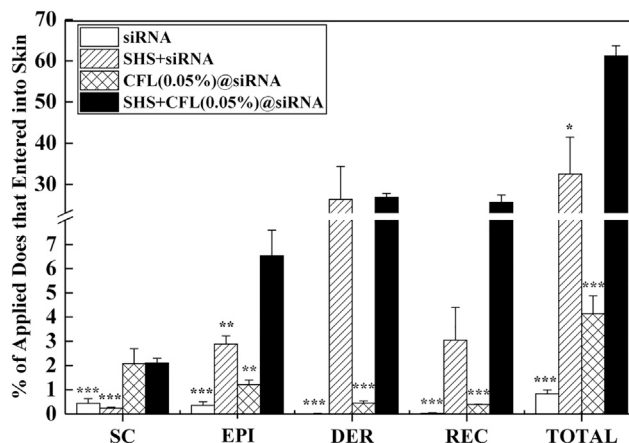


**Figure 3. GAPDH-siRNA Penetrates Different Skin Layer *In Vitro***

SC represents the first to the tenth tape strip, EPI represents the epidermis, DER represents the dermis, REC represents the receptor. Values represent mean  $\pm$  SD (n = 3). \*p < 0.05; \*\*p < 0.01; \*\*\*p < 0.001.

SHS in combination with CFL(0.05%) to topically deliver GAPDH-siRNA into skin of female BALB/C mice (7–8 weeks). The CFL carrying GAPDH-siRNA was delivered into mice skin by subcutaneous injection and SHS treatment. In the case of the subcutaneous injection group, while there was no significant difference between the GAPDH protein knockdown in the injection center ( $26.17\% \pm 6.25\%$ ) and 0.5 cm away from the injection center ( $26.38\% \pm 7.40\%$ ), the GAPDH protein knockdown dropped rapidly in the position of 1 cm away from the injection center ( $6.45\% \pm 5.87\%$ ; Figure 8). In contrast, the topical application of SHS in combination with CFL(0.05%) on mice over 72 h led to  $29.21\% \pm 1.41\%$  of GAPDH knockdown in the entire topically applied area, which was significantly higher than that from SHS treatment alone ( $5.48\% \pm 7.97\%$ ,  $p < 0.01$ ) and was comparable to that from the subcutaneous injection of CFL(0.05%)@siRNA mixture in the injection center area ( $26.17\% \pm 6.25\%$ ,  $p = 0.458$ ) (Figure 8). These results indicated that the utilization of SHS in combination with CFL(0.05%) is a promising delivery system for the topical application of RNAi therapy *in vivo*.

### DISCUSSION

SHS can create plenty of new long-lasting micro-channels through or into the SC and subsequently facilitate the penetration of drug or nano-particles into deep skin layers. Thus, the skin penetration of CFL containing siRNA induced by the SHS is significantly enhanced compared to that induced by the Dermaroller (HC902, 162 microneedles, 0.2 mm, Munich, Germany;  $p < 0.01$ ; Figures 2, 4G, and 4H), supporting our previous conclusion that SHS can be used as a more effective microneedle to topically deliver therapeutics and even nano-carriers system such as CFL.

Further, SHS is safe to be topically applied as a novel microneedle for the skin drug delivery. The microchannels created by SHS are the gaps between skin and SHS within SC layer. We believe that these gaps are nano-scale since rigid conventional liposomes (around 100 nm)

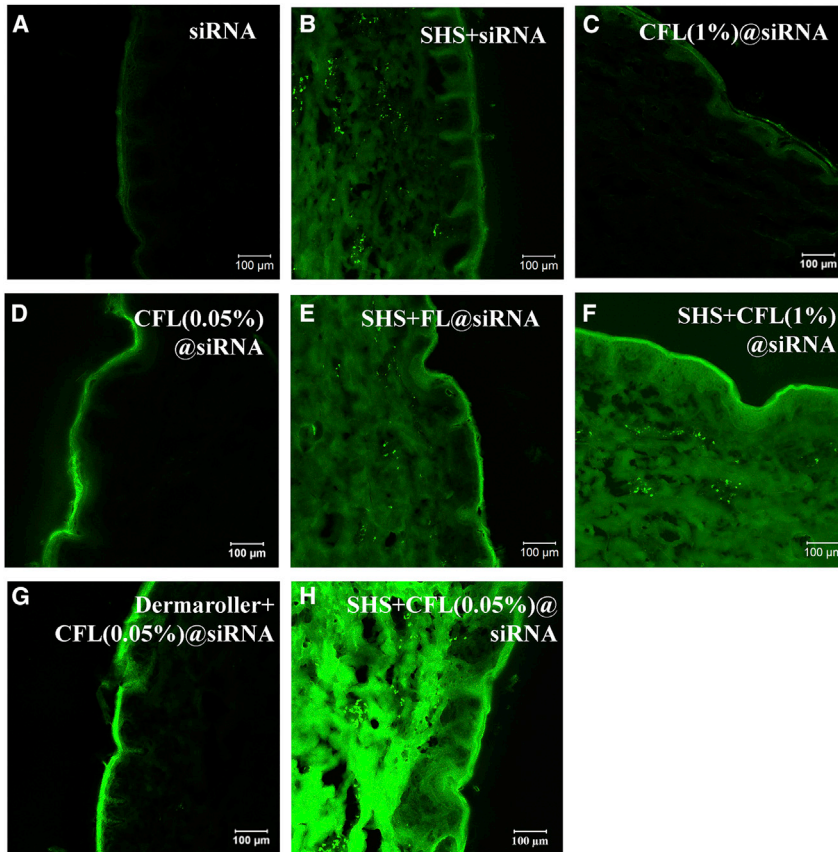


**Figure 4. Visualization of Skin Delivery of siRNA Induced by Different Formulations**

(A) siRNA alone. (B) Topical application of SHS and siRNA. (C) Topical application of CFL (1%) containing siRNA. (D) Topical application of CFL (0.05%) containing siRNA. (E) siRNA with SHS and FL treatment. (F) siRNA with SHS and CFL (1%) treatment. (G) siRNA with dermaroller and CFL (0.05%) treatment. (H) siRNA with SHS and CFL (0.05%) treatment.

microchannels caused by SHS are gradually closed. Moreover, transepidermal water loss and guinea pig skin irritation experiments in our previous study have verified the safety of SHS topical treatment, and skin disruption caused by SHS treatment can be repaired with time and efficiency.<sup>38,39</sup> Therefore, there should be low risk or no risk of most bacterial or virus infection after SHS topical treatment.

Subcutaneous injection could be the most direct method to deliver siRNA into skin viable tissue layers; it is also commonly used as a positive control to evaluate the efficacy of skin delivery technologies for therapeutics such as siRNA. From the *in vivo* results, the RNAi efficiency induced by subcutaneous injection of CFL containing siRNA is inversely proportional to the distance to the injection center (Figure 8). In addition,

cannot pass through these microchannels according to our recent study.<sup>39</sup> Subsequently, while SHS can be gradually eliminated from the skin with desquamation and eventually leaves the skin, the skin

subcutaneous injection may lead to significant patient non-compliance due to the severe needle-phobia.<sup>40</sup> In contrast, the RNAi efficiency induced by the topical administration of SHS combined with

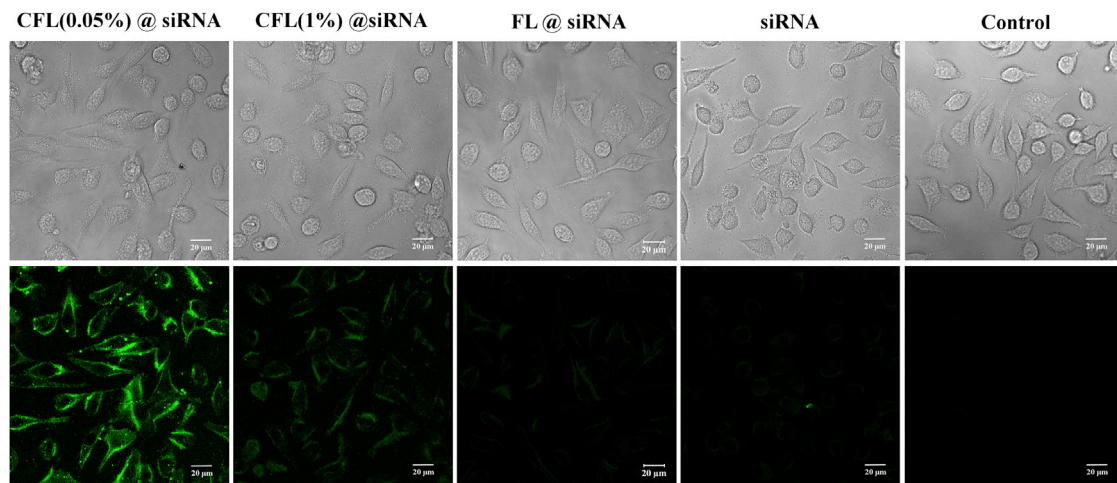


**Figure 5. CFL(0.05%) Obviously Facilitate the Internalization of FAM-GAPDH siRNA in L929 Cell Compared to Other Lipid Vesicles**

Cells for transfection were incubated in 24-well plates. The up line shows an image of the L929 cell in bright field. The bottom line shows the internalization of siRNA in cells under different liposome treatments.

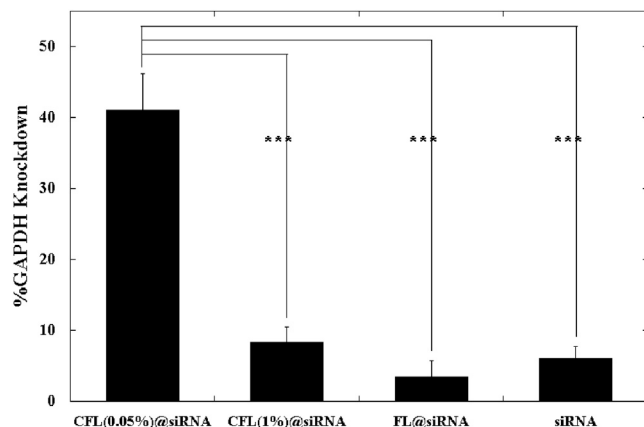


**Figure 6. Liposome Induced Knockdown of GAPDH Protein in L929 Cell**

Cells for transfection were incubated in 24-well plates. CFL(0.05%)@siRNA: add 1.5  $\mu$ L of CFL(0.05%) and 30 pmol of GAPDH siRNA mixture to each well; CFL(1%)@siRNA: add 1.5  $\mu$ L of CFL(1%) and 30 pmol of GAPDH siRNA mixture to each well; FL@siRNA: add 1.5  $\mu$ L of FL and 30 pmol of GAPDH siRNA mixture to each well; siRNA: 30 pmol/well GAPDH-siRNA. Values represent mean  $\pm$  SD (n = 6). \*\*\*p < 0.001.

CFL is not only comparative to that of the subcutaneous injection center area ( $p = 0.458$ ), but also almost equally and homogeneously available to all topically applied area (Figure 8). These results suggest that the utilization of SHS in combination with CFL can be suitable for large-area topical application for RNAi therapy.

Since naked RNA cannot penetrate the cell lipid membrane, many strategies have been developed to address the skin delivery of siRNA.<sup>6,41–46</sup> siRNA can be protected from degradation by lipid vesicles<sup>47</sup> and consequently have been delivered into cells by lipid vesicles for almost 2 decades.<sup>48</sup> In this study, different lipid vesicles, including cationic flexible liposome (CFL) and flexible liposome (FL) were used to deliver siRNA into skin. Without SHS, these lipid vesicles only increased the distribution of siRNA in skin upper layers (Figure 3). In contrast, SHS creates plenty of microchannels on the skin to facilitate the skin penetration of lipid vesicles with a hydration-driven transport mechanism.<sup>38</sup> The synergistic effect from the SHS and lipid vesicles also appears to be proportional to the vesicles' deformability. The flexibility of liposomes can be adjusted by modifying the concentration of surfactants,<sup>49,50</sup> solvent in the system,<sup>51</sup> and even lipid concentration as demonstrated in this study. The well-designed flexible liposomes, such as CFL(0.05%), can squeeze into skin through the microchannels created by SHS with carrying vesicle-bound siRNA into deep skin layers under the driving force of transdermal osmotic gradients.

Further, once the siRNA is delivered into the skin, it must also be ensured that the siRNA can be delivered into the viable cells. While both CFL(1%) and FL show high cytotoxicity with resulting in low knockdown efficiency of target gene, CFL(0.05%) can significantly increase the cell entry of siRNA (Figure 5) with the low cytotoxicity (Figure 7), which in turn led to the improved GAPDH knockdown efficiency.

The silencing of siRNA for specific pathogenic genes sequences has led to a large number of preclinical and even clinical studies.<sup>52</sup> However, two barriers posed by the stratum corneum and viable skin cells membrane limits the entering of siRNA into viable skin cells. The topical application of SHS in combination with CFL in the skin delivery of siRNA may open new opportunities to siRNA-based treatment for dermatological diseases.

## Conclusions

This study demonstrated that the combined use of SHS and well-designed CFL, CFL(0.05%), significantly enhanced the skin penetration and deposition of siRNA into deep skin layers. Cell transfection experiments *in vitro* showed that CFL(0.05%) as a siRNA carrier system resulted in a significant decrease in the expression of GAPDH protein in the cells. *In vivo* experiments further confirmed the effectiveness of the combined use of SHS and CFL(0.05%) for the delivery of siRNA into skin viable cells, which in turn can effectively silence the target gene expression. The topical application of SHS in combination with a well-designed CFL, such as CFL(0.05%), could be a platform technology for topical RNAi therapy.

## MATERIALS AND METHODS

### Chemicals

2, 3-dioleoyloxy-propyl-trimethylammoniumchlorid (DOTAP) was purchased from CordenPharma (Switzerland). Phospholipon 90G was purchased from Lipoid GmbH (Germany). Thiazolyl Blue Tetrazolium Bromide (MTT) and BRIJ O20 were purchased from Sigma-Aldrich (St. Louis Missouri, USA). FAM-labeled GAPDH-siRNA (5'-FAM-CACUCAAGAUUGUCAGCAATT-3') was obtained from GenePharma (Shanghai, China). Neutral Balsam was purchased from Solarbio (Beijing, China). L929 cell was purchased from iCell Bioscience (Shanghai, China). Trypsin 0.25% (1 $\times$ ) Solution, Dulbecco's modified Eagle's medium (DMEM)/high glucose, and 100 $\times$  penicillin/streptomycin solution were purchased from HyClone (Logan City, UT, USA). Fetal bovine serum (FBS) and opti-mem (1 $\times$ ) were purchased from GIBCO (Grand Island, USA). Chloral hydrate was purchased from Macklin (Shanghai, China). KAlert GAPDH Assay was purchased from Thermo Scientific (USA). Female BALB/c mice (6–7 weeks old) were purchased from Xiamen University Laboratory Animal Center. All other chemicals (analytical grade) used in this study were purchased from Sinopharm Group (Shanghai, China).

### Preparation of Lipid Vesicle Formulations

In this study, CFL and FL were prepared using thin film hydration methods.<sup>53,54</sup> DOTAP (10 mg/mL) with BRIJ O20 (12 mg/mL; CFL) or 90G (40 mg/mL) with BRIJ O20 (12 mg/mL; FL) were dissolved in chloroform. The solvent was then removed by using a rotary evaporator at 25 $^{\circ}$ C. The obtained lipids film was hydrated with 0.2 M PBS (pH = 7.4; FL) or the solution of 0.2 M Tris-HCl (pH = 4; CFL). The obtained suspension was then homogenized with a liposome extruder (LiposoFast, AVESTIN) and the polycarbonate film (100 nm). To optimize the ratio between CFL and siRNA, we further diluted the original CFL with diethylpyrocarbonate (DEPC) water to adjust the concentration of liposomal particles. Different CFL or FL were mixed with siRNA

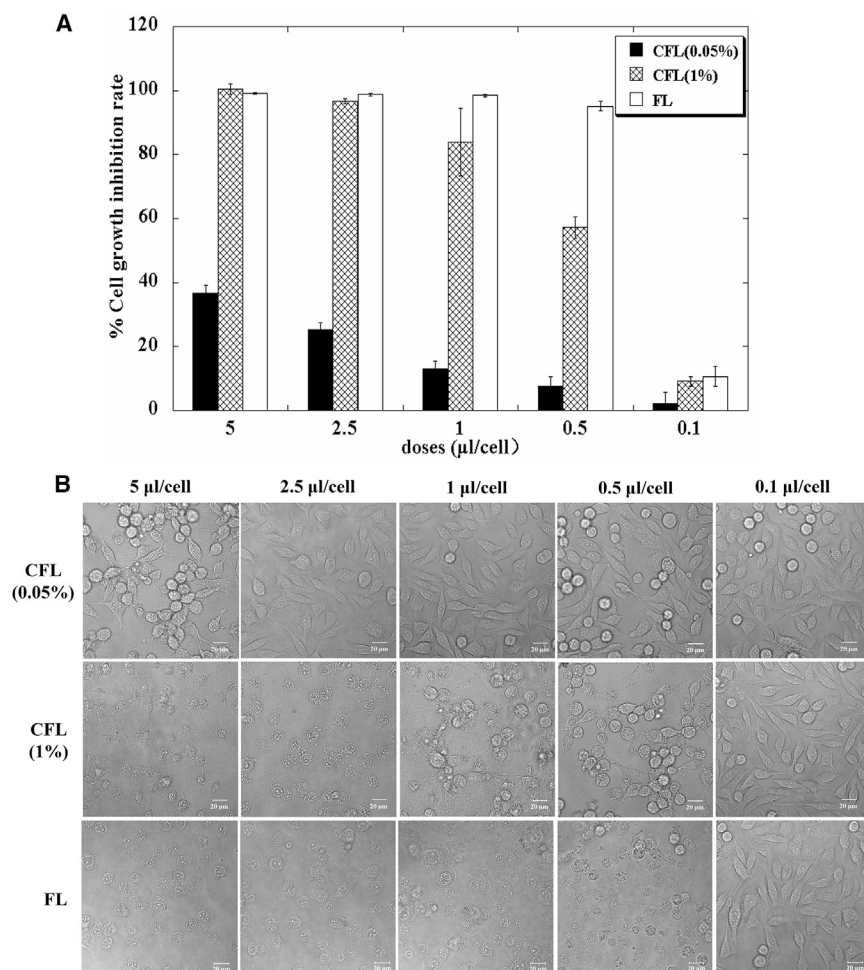


**Figure 7. Cytotoxicity of Liposomes to Cells (L929)**

(A) The growth inhibition rate of cells after adding different doses of CFL (0.05%), CFL (1%), and FL. Values represent mean  $\pm$  SD (n = 6). (B) Cell growth status after adding different doses of liposomes. The first line shows the morphological change of L929 cells after adding different doses of CFL (0.05%). The second line shows the morphological change of L929 cells after different doses of CFL (1%) were added. The third line shows the morphological change of L929 cells after adding different doses of FL. The dosages were 5  $\mu$ L/cell, 2.5  $\mu$ L/cell, 1  $\mu$ L/cell, 0.5  $\mu$ L/cell, and 0.1  $\mu$ L/cell, respectively.

(25 nmol/mL) and then ultrasonic treatment for 20 min to prepare CFL@FAM-siRNA and FL@FAM-siRNA formulations.

### Preparation and Purification of SHS

The raw material of SHS was obtained from marine sponge *Haliclona* sp. that was cultured explants cultivated in 2018 at Dongshan Bay (Zhangzhou, Fujian Province, China). The purified SHS (>95%, w/w) was prepared and purified as described in our patent (ZL201610267764.6).

### Characterization of Lipid Vesicles

The lipid vesicles with or without siRNA were characterized in terms of particle size, polydispersity index (PDI) and  $\zeta$ -potential by using a Malvern Zetasizer Nano ZS90 instrument (Malvern Instruments, UK). The deformability of different lipid vesicles was determined in accordance with previous study.<sup>55</sup> The time of test formulation to pass through a polycarbonate film (100 nm of pore size) at a pressure of 0.25 MPa was recorded as Tw, Tc, and Tf for water, CFL, and FL, respectively. The deformability of lipid vesicles was calculated as follows:

$$\text{Deformability}(\%) = \frac{T_w}{T_c \text{ or } T_f} \times 100\%$$

The lipid vesicles were further visualized by using a transmission electron microscope (TEM, FEI Tecnai G2 Spirit BioTwin, Hillsboro, USA). Prior to the analysis, 10  $\mu$ L of lipid vesicles were applied onto copper grids. The samples were then stained by uranyl acetate and dried on air. Finally, the sample was observed by the TEM at an operating voltage of 120 KV.

### Skin Penetration Study *In Vitro*

The porcine skin (YinXiang Group, Xiamen, China) was used for *in vitro* penetration study. The skin was prepared as described in the previous study.<sup>38</sup> Briefly, the subcutaneous fatty tissue under the porcine skin was removed carefully with a scalpel. The hair shaft was shaved to less than 5 mm using an electric razor (Codos KP-3000, Guangzhou, China). The porcine skin was then cleaned with ultrapure water and stored at  $-20^\circ\text{C}$ . Skin was thawed at room temperature before use. *In vitro*, the skin was punched out in disk samples

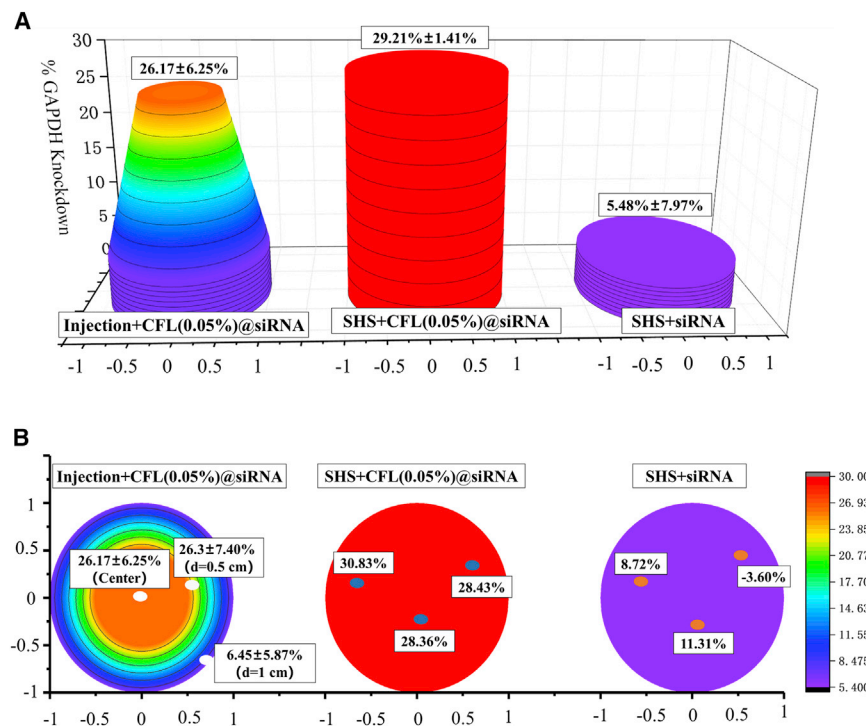


**Figure 8. The Knockdown of GAPDH Protein Induced by Different siRNA Delivery after 72 H Treatment *In Vivo***

(A) 3D simulation of GAPDH protein knockdown rate. (B) Top view of (A). Formulations of all group contain 25 nmol/mL of GAPDH-siRNA. Injection + CFL(0.05%)@siRNA: the formulation contains 50  $\mu$ L of CFL and 25 nmol/mL of GAPDH-siRNA, subcutaneous injection. The knockdown of GAPDH protein at three different locations in the Injection + CFL(0.05%)@siRNA group was determined, the center location of the injection, a location of 0.5 cm from the center of the injection, and a location of 1 cm from the center of the injection. SHS + CFL(0.05%)@siRNA: the formulation contains 50  $\mu$ L of CFL and 25 nmol/mL of GAPDH-siRNA, SHS massage; GAPDH protein knockdown rate was measured at three random sites in the siRNA delivery area. SHS: The formulation only contains 25 nmol/mL of GAPDH-siRNA, SHS massage; GAPDH protein knockdown rate was measured at three random sites in the siRNA delivery area. Values indicate mean  $\pm$  SE (n = 3).

(36 mm) and put in vertical Franz diffusion cells (FDCs, ZhengTong, Tianjin, China). The effective penetration area was 1.77 cm<sup>2</sup>. The receptor compartment (12 mL) was filled with deaerated phosphate buffered saline (PBS, pH 7.4, 20 mM) and then placed in a water bath at 37°C  $\pm$  0.5°C. The conductivity of the skin was measured before the penetration study to ensure the integrity of the skin barrier.<sup>38</sup> SHS (5 mg/cm<sup>2</sup>) were topically applied to skin by using a homemade electric applicator (application force of about 0.3N and massage speed of around 300 r/min) for 2 min. After the application, the skin was washed with PBS (0.2 M, pH = 7.4) to remove residual SHS on the skin. The test formulations (150  $\mu$ L) were then applied non-occlusively on the skin surface. Each group was assessed at least in triplicate. The penetration time of all test formulations was over 16 h. The receptor phase solution was withdrawn at the end of penetration study. The concentration of the FAM-labeled siRNA (with an excitation wavelength of 485 nm and an emission wavelength of 520 nm) in solution was measured by a microplate reader (Infinite M200 Pro, Switzerland). The linearity of the standard curve was verified of accuracy ( $R^2 = 0.9999$ ). The skin was washed with 0.2 M PBS (pH = 7.4) and tapped dry to remove the test formulations left for the further skin separation treatment.

#### Extraction of FAM-siRNA Skin Deposition

The skin SC layer was separated from the skin by using the tape-stripping method.<sup>56</sup> Briefly, the SC was stripped 10 times continuously using transparent tapes (Scotch Transparent Tape, 3M Corporation, USA). The viable epidermis left was then peeled off from the dermis. The obtained viable epidermis and dermis tissue was cut into small pieces. The individual skin tissues were placed in brown avoid-light

glass bottles and placed in a shaker (25°C, 200 rpm/min) overnight. The FAM-labeled siRNA accumulated in each skin layer was extracted with methanol/PBS mixture (v/v, 1:1). All liquid supernatant in the bottles was obtained by centrifugation (8,000 r/min, 5 min, H1650-W, XiangYi Centrifuge Instrument, Changsha, China) to determine the FAM-labeled siRNA deposition in different skin layers. The FAM-labeled siRNA was measured with the microplate reader. The linearity of the standard curve was confirmed ( $R^2 = 0.9999$ ).

#### Skin Imaging Studies

The distribution of FAM-siRNA in the skin was studied using a confocal microscopy (LSM780NLO, Carl Zeiss, Germany). Skin biopsies (5 mm) were punched out and frozen rapidly in the OCT compound (Sakura Finetek, USA). The obtained biopsies were cut into a section (20  $\mu$ m of thickness) by a freezing microtome (CM1900, Leica, Germany). The obtained sample was placed on adhesive glass slide with 50  $\mu$ L of neutral balsam (Solarbio, Beijing, China) and a coverslip placed thereon for the further imaging.

#### Cell Culturing

L929 cell (mouse fibroblasts) were grown in DMEM/high glucose medium containing 100 U/mL penicillin, 100  $\mu$ g/mL streptomycin, and 10% FBS (GIBCO). The cells were cultured in a humidified incubator containing 5% CO<sub>2</sub> at 37°C.

#### Cytotoxicity of Lipid Vesicles

L929 cells were seeded in 96-well plates (1  $\times$  10<sup>4</sup> cells/well) at 37°C for 1 day. The medium in each well was removed and replaced with fresh one. The cells were then incubated at 37°C for another 1 day with a series of different doses of lipid vesicles (5.0  $\mu$ L/well, 2.5  $\mu$ L/well, 1.0  $\mu$ L/well, 0.5  $\mu$ L/well, 0.1  $\mu$ L/well). Thereafter, 10  $\mu$ L of MTT

reagent (5 mg/mL) was added to each well and incubated with L929 cells at 37°C and 5% CO<sub>2</sub> for 4 h. Finally, the medium, lipid vesicles and MTT mixture in each well was removed and replaced with 150 µL of DMSO. The plates were placed in a shaker (150 rpm/min) for 10 min. Finally, the absorbance of the solution in each well was measured at 490 nm. The inhibition rate of different lipid vesicles to cells and the corresponding IC<sub>50</sub> were calculated according to the absorbance.

#### GAPDH Protein Knockdown *In Vitro*

L929 cells were seeded in 24-well plates (5 × 10<sup>5</sup> cells/well) at 37°C with 5% CO<sub>2</sub>. Transfection experiments were carried out until the density of cells were about 70%–80%. 1.5 µL of different lipid vesicles and 3 µL of FAM-siRNA (10 nmol/mL) were mixed thoroughly with 25 µL of opti-mem. The obtained mixture was allowed to stand at 25°C for 5 min and then added to each well. The cells were incubated for 6 h in an incubator. The imaging of transfection was performed using a confocal microscope (LSM780NLO, Carl Zeiss, Germany). Transfection mixture was added to each well and incubated for 68 h. The GAPDH protein expression level was determined with a KDa-Alert GAPDH Assay Kit and the knockdown rate was calculated. There are six repetitions in each group.

#### Skin Penetration *In Vivo*

Female BALB/c mice (6 weeks old) were purchased from the Laboratory Animal Center (Xiamen University, China) and used in skin delivery of siRNA *in vivo*. Based on protocols approved by the Institutional Animal Care and Use Committee at Xiamen University Laboratory Animal Center, we investigated the effect of different lipid vesicles on the knockdown of GAPDH protein *in vivo*. A total of four groups were designed: subcutaneous injection of CFL(0.05%)@siRNA as a positive control; topical application of SHS combined use with CFL(0.05%)@siRNA; topical application of SHS and siRNA; and topical application of a negative siRNA control. In the case of the subcutaneous injection group, 50 µL of CFL (0.05%) was mixed thoroughly with 100 µL of siRNA (3.75 nmol) solution, and then the mixture was injected subcutaneously into mice. In the case of SHS treatment groups, mice were intraperitoneally injected with 150 µL of chloral hydrate (4%) for anesthesia. The hair on the back of the mice was clipped to prepare an exposed skin area of 1.77 cm<sup>2</sup>. The exposed skin was then massaged using SHS (5 mg/cm<sup>2</sup>) for 2 min with the application force of 0.3 N. The treatment area was then washed 3 times with PBS (0.2 M, pH = 7.4) to remove SHS. For the topical application of SHS combined with CFL-siRNA group, a mixed solution of 50 µL of CFL (0.05%) and 100 µL of siRNA (3.75 nmol) solution was dropped on the treatment area non-occlusively. For the SHS group, 150 µL of siRNA (3.75 nmol) solution was applied on the SHS treatment area occlusively. For the control group, 150 µL of a negative control siRNA (3.75 nmol) solution was applied on the exposed skin area occlusively. The mice were sacrificed by CO<sub>2</sub> overexposure after 72 h. Mice skin tissues were collected from the treated area, and GAPDH protein expression levels were determined using KDaAlert GAPDH Assay Kit. Each set of experiments comprised three repetitions.

#### Statistical Analysis

All data in this study were presented as mean ± SD. All experiments were investigated at least in triplicate. Statistical significance was determined by the two-tailed and unpaired Student's t test in IBM SPSS Statistics 19. A p < 0.05 is considered to be significantly different.

#### AUTHOR CONTRIBUTIONS

M.C. and J.C. designed the experiments. X.L., J.Z., and H.O. performed the experiments. X.L. and M.C. wrote the article with the help of S.M.

#### CONFLICTS OF INTEREST

The authors declare no competing interests.

#### ACKNOWLEDGMENTS

This work was financially supported by Marine Economic Development Subsidy Project of Fujian Province, China (grant number FJHJF-L-2019-03) and Science and Technology Planning Project of Fujian Province, China (grant number 2017Y4015). We thank Chi Zhang for assistance with intraperitoneal injections, Luming Yao and Qingbing Zheng for assistance with TEM study, Caiming Wu for assistance with SEM study, Huiyun Chen for assistance with confocal microscopy study, and Saiman Zhang for assistance with the preprocessing of porcine skin.

#### REFERENCES

1. Fire, A., Xu, S., Montgomery, M.K., Kostas, S.A., Driver, S.E., and Mello, C.C. (1998). Potent and specific genetic interference by double-stranded RNA in *Caenorhabditis elegans*. *Nature* 391, 806–811.
2. Elbashir, S.M., Harborth, J., Lendeckel, W., Yalcin, A., Weber, K., and Tuschl, T. (2001). Duplexes of 21-nucleotide RNAs mediate RNA interference in cultured mammalian cells. *Nature* 411, 494–498.
3. Chong, R.H., Gonzalez-Gonzalez, E., Lara, M.F., Speaker, T.J., Contag, C.H., Kaspar, R.L., Coulman, S.A., Hargest, R., and Birchall, J.C. (2013). Gene silencing following siRNA delivery to skin via coated steel microneedles: In vitro and in vivo proof-of-concept. *J. Control. Release* 166, 211–219.
4. Nakamura, M., Jo, J., Tabata, Y., and Ishikawa, O. (2008). Controlled delivery of T-box21 small interfering RNA ameliorates autoimmune alopecia (Alopecia Areata) in a C3H/HeJ mouse model. *Am. J. Pathol.* 172, 650–658.
5. Jakobsen, M., Stenderup, K., Rosada, C., Moldt, B., Kamp, S., Dam, T.N., Jensen, T.G., and Mikkelsen, J.G. (2009). Amelioration of psoriasis by anti-TNF-alpha RNAi in the xenograft transplantation model. *Mol. Ther.* 17, 1743–1753.
6. Inoue, T., Sugimoto, M., Sakurai, T., Saito, R., Futaki, N., Hashimoto, Y., Honma, Y., Arai, I., and Nakaike, S. (2007). Modulation of scratching behavior by silencing an endogenous cyclooxygenase-1 gene in the skin through the administration of siRNA. *J. Gene Med.* 9, 994–1001.
7. Ishimoto, T., Takei, Y., Yuzawa, Y., Hanai, K., Nagahara, S., Tarumi, Y., Matsuo, S., and Kadomatsu, K. (2008). Downregulation of monocyte chemoattractant protein-1 involving short interfering RNA attenuates hapten-induced contact hypersensitivity. *Mol. Ther.* 16, 387–395.
8. Nakai, N., Kishida, T., Shin-Ya, M., Imanishi, J., Ueda, Y., Kishimoto, S., and Mazda, O. (2007). Therapeutic RNA interference of malignant melanoma by electrotransfer of small interfering RNA targeting Mitf. *Gene Ther.* 14, 357–365.
9. Nakai, N., Kishida, T., Hartmann, G., Katoh, N., Imanishi, J., Kishimoto, S., and Mazda, O. (2010). Mitf silencing cooperates with IL-12 gene transfer to inhibit melanoma in mice. *Int. Immunopharmacol.* 10, 540–545.
10. Leachman, S.A., Hickerson, R.P., Schwartz, M.E., Bullough, E.E., Hutcherson, S.L., Boucher, K.M., Hansen, C.D., Eliason, M.J., Srivatsa, G.S., Kornbrust, D.J., et al.



- (2010). First-in-human mutation-targeted siRNA phase Ib trial of an inherited skin disorder. *Mol. Ther.* 18, 442–446.
11. Kim, J.Y., Shin, J.Y., Kim, M.R., Hann, S.K., and Oh, S.H. (2012). siRNA-mediated knock-down of COX-2 in melanocytes suppresses melanogenesis. *Exp. Dermatol.* 21, 420–425.
  12. Prausnitz, M.R., Mitragotri, S., and Langer, R. (2004). Current status and future potential of transdermal drug delivery. *Nat. Rev. Drug Discov.* 3, 115–124.
  13. Brown, M.B., Martin, G.P., Jones, S.A., and Akomeah, F.K. (2006). Dermal and transdermal drug delivery systems: current and future prospects. *Drug Deliv.* 13, 175–187.
  14. Peter, M., and Elias, M.D. (1983). Epidermal Lipids, Barrier Function, and Desquamation. *J. Invest. Dermatol.* 80, 44s–49s.
  15. Cevc, G., and Vierl, U. (2010). Nanotechnology and the transdermal route: A state of the art review and critical appraisal. *J. Control. Release* 141, 277–299.
  16. Tuan-Mahmood, T.M., McCrudden, M.T., Torrisi, B.M., McAlister, E., Garland, M.J., Singh, T.R., and Donnelly, R.F. (2013). Microneedles for intradermal and transdermal drug delivery. *Eur. J. Pharm. Sci.* 50, 623–637.
  17. Li, H., Low, Y.S., Chong, H.P., Zin, M.T., Lee, C.Y., Li, B., Leolukman, M., and Kang, L. (2015). Microneedle-Mediated Delivery of Copper Peptide Through Skin. *Pharm. Res.* 32, 2678–2689.
  18. Pham, Q.D., Bjorklund, S., Engblom, J., Topgaard, D., and Sparr, E. (2016). Chemical penetration enhancers in stratum corneum - Relation between molecular effects and barrier function. *J. Control. Release* 232, 175–187.
  19. Rigon, R.B., Fachinetti, N., Severino, P., Santana, M.H., and Chorilli, M. (2016). Skin Delivery and in Vitro Biological Evaluation of Trans-Resveratrol-Loaded Solid Lipid Nanoparticles for Skin Disorder Therapies. *Molecules* 21, E116.
  20. Desai, P.R., Marepally, S., Patel, A.R., Voshavar, C., Chaudhuri, A., and Singh, M. (2013). Topical delivery of anti-TNF $\alpha$  siRNA and capsaicin via novel lipid-polymer hybrid nanoparticles efficiently inhibits skin inflammation in vivo. *J. Control. Release* 170, 51–63.
  21. Rajendran, L., Knölker, H.J., and Simons, K. (2010). Subcellular targeting strategies for drug design and delivery. *Nat. Rev. Drug Discov.* 9, 29–42.
  22. Neumann, E., Schaefer-Ridder, M., Wang, Y., and Hofschneider, P.H. (1982). Gene transfer into mouse lymphoma cells by electroporation in high electric fields. *EMBO J* 1, 841–845.
  23. Aigner, A. (2006). Delivery systems for the direct application of siRNAs to induce RNA interference (RNAi) in vivo. *J. Biomed. Biotechnol.* 2006, 71659.
  24. Love, T.M., Moffett, H.F., and Novina, C.D. (2008). Not miR-ly small RNAs: big potential for microRNAs in therapy. *J. Allergy Clin. Immunol.* 121, 309–319.
  25. van der Rest, M.E., Lange, C., and Molenaar, D. (1999). A heat shock following electroporation induces highly efficient transformation of *Corynebacterium glutamicum* with xenogenic plasmid DNA. *Appl. Microbiol. Biotechnol.* 52, 541–545.
  26. Park, D., Song, G., Jo, Y., Won, J., Son, T., Cha, O., Kim, J., Jung, B., Park, H., Kim, C.W., and Seo, J. (2016). Sonophoresis Using Ultrasound Contrast Agents: Dependence on Concentration. *PLoS ONE* 11, e0157707.
  27. Zhang, D., Das, D.B., and Rielly, C.D. (2014). Microneedle assisted micro-particle delivery from gene guns: experiments using skin-mimicking agarose gel. *J. Pharm. Sci.* 103, 613–627.
  28. Singh, N.D., and Banga, A.K. (2013). Controlled delivery of ropinirole hydrochloride through skin using modulated iontophoresis and microneedles. *J. Drug Target.* 21, 354–366.
  29. Song, C.K., Balakrishnan, P., Shim, C.K., Chung, S.J., Chong, S., and Kim, D.D. (2012). A novel vesicular carrier, transthesosome, for enhanced skin delivery of voriconazole: characterization and in vitro/in vivo evaluation. *Colloids Surf. B Biointerfaces* 92, 299–304.
  30. Ishii, H., Suzuki, T., Todo, H., Kamimura, M., and Sugibayashi, K. (2011). Iontophoresis-facilitated delivery of prednisolone through throat skin to the trachea after topical application of its succinate salt. *Pharm. Res.* 28, 839–847.
  31. Ogura, M., Paliwal, S., and Mitragotri, S. (2008). Low-frequency sonophoresis: current status and future prospects. *Adv. Drug Deliv. Rev.* 60, 1218–1223.
  32. Choi, S.Y., Kwon, H.J., Ahn, G.R., Ko, E.J., Yoo, K.H., Kim, B.J., Lee, C., and Kim, D. (2017). Hyaluronic acid microneedle patch for the improvement of crow's feet wrinkles. *Dermatol. Ther. (Heidelb.)* 30, 12546.
  33. Ita, K. (2017). Recent progress in transdermal sonophoresis. *Pharm. Dev. Technol.* 22, 458–466.
  34. Ita, K. (2016). Transdermal iontophoretic drug delivery: advances and challenges. *J. Drug Target.* 24, 386–391.
  35. Yang, G., Zhang, Y., and Gu, Z. (2018). Punching and Electroporation for Enhanced Transdermal Drug Delivery. *Theranostics* 8, 3688–3690.
  36. Bochicchio, S., Dalmoro, A., Barba, A.A., Grassi, G., and Lamberti, G. (2014). Liposomes as siRNA delivery vectors. *Curr. Drug Metab.* 15, 882–892.
  37. Ita, K.B. (2015). Chemical Penetration Enhancers for Transdermal Drug Delivery - Success and Challenges. *Curr Drug Deliv* 12, 645–651.
  38. Zhang, S., Ou, H., Liu, C., Zhang, Y., Mitragotri, S., Wang, D., and Chen, M. (2017). Skin Delivery of Hydrophilic Biomacromolecules Using Marine Sponge Spicules. *Mol. Pharm.* 14, 3188–3200.
  39. Zhang, C., Zhang, K., Zhang, J., Ou, H., Duan, J., Zhang, S., Wang, D., Mitragotri, S., and Chen, M. (2019). Skin delivery of hyaluronic acid by the combined use of sponge spicules and flexible liposomes. *Biomater. Sci.* 7, 1299–1310.
  40. Li, J., Li, X., Zhang, Y., Zhou, X.K., Yang, H.S., Chen, X.C., Wang, Y.S., Wei, Y.Q., Chen, L.J., Hu, H.Z., and Liu, C.Y. (2010). Gene therapy for psoriasis in the K14-VEGF transgenic mouse model by topical transdermal delivery of interleukin-4 using ultradeformable cationic liposome. *J. Gene Med.* 12, 481–490.
  41. Kazemi Oskuee, R., Mahmoudi, A., Gholami, L., Rahmatkhan, A., and Malaekhe-Nikouei, B. (2016). Cationic Liposomes Modified with Polyallylamine as a Gene Carrier: Preparation, Characterization and Transfection Efficiency Evaluation. *Adv. Pharm. Bull.* 6, 515–520.
  42. Shah, P.P., Desai, P.R., Channer, D., and Singh, M. (2012). Enhanced skin permeation using polyarginine modified nanostructured lipid carriers. *J. Control. Release* 161, 735–745.
  43. Whitehead, K.A., Langer, R., and Anderson, D.G. (2009). Knocking down barriers: advances in siRNA delivery. *Nat. Rev. Drug Discov.* 8, 129–138.
  44. Zhang, S., Zhao, B., Jiang, H., Wang, B., and Ma, B. (2007). Cationic lipids and polymers mediated vectors for delivery of siRNA. *J. Control. Release* 123, 1–10.
  45. Wang, J., Hu, J.H., Li, F.Q., Liu, G.Z., Zhu, Q.G., Liu, J.Y., Ma, H.J., Peng, C., and Si, F.G. (2007). Strong cellular and humoral immune responses induced by transcutaneous immunization with HBsAg DNA-cationic deformable liposome complex. *Exp. Dermatol.* 16, 724–729.
  46. Bouwstra, J.A., Honeywell-Nguyen, P.L., Gooris, G.S., and Ponec, M. (2003). Structure of the skin barrier and its modulation by vesicular formulations. *Prog. Lipid Res.* 42, 1–36.
  47. Yu, B., Zhao, X., Lee, L.J., and Lee, R.J. (2009). Targeted delivery systems for oligonucleotide therapeutics. *AAPS J.* 11, 195–203.
  48. Niemiec, S.M., Latta, J.M., Ramachandran, C., Weiner, N.D., and Roessler, B.J. (1997). Perifollicular transgenic expression of human interleukin-1 receptor antagonist protein following topical application of novel liposome-plasmid DNA formulations in vivo. *J. Pharm. Sci.* 86, 701–708.
  49. Hussain, A., Singh, S., Sharma, D., Webster, T.J., Shafaat, K., and Faruk, A. (2017). Elastic liposomes as novel carriers: recent advances in drug delivery. *Int. J. Nanomedicine* 12, 5087–5108.
  50. Jain, S., Patel, N., Shah, M.K., Khatri, P., and Vora, N. (2017). Recent Advances in Lipid-Based Vesicles and Particulate Carriers for Topical and Transdermal Application. *J. Pharm. Sci.* 106, 423–445.
  51. Das, S.K., Chakraborty, S., Roy, C., Rajabalaya, R., Mohaimin, A.W., Khanam, J., Nanda, A., and David, S.R. (2018). Ethosomes as Novel Vesicular Carrier: An Overview of the Principle, Preparation and its Applications. *Curr. Drug Deliv.* 15, 795–817.
  52. Geusens, B., Lambert, J., De Smedt, S.C., Buyens, K., Sanders, N.N., and Van Gele, M. (2009). Ultradeformable cationic liposomes for delivery of small interfering RNA (siRNA) into human primary melanocytes. *J. Control. Release* 133, 214–220.

53. Kaisheva, M., Alexandrova, L., Spassov, I., and Diakova, B. (2001). Investigation of thin films formed from liposome suspensions on quartz substrate. *Colloids Surf. B Biointerfaces* 20, 137–143.
54. Bendas, E.R., and Tadros, M.I. (2007). Enhanced transdermal delivery of salbutamol sulfate via ethosomes. *AAPS PharmSciTech* 8, E107.
55. Bing, T., and Tang, N. (2013). Preparation and related properties of human epidermal active factor flexible nanoliposomes. *China Pharmaceuticals* 22, 12–14.
56. Chen, M., Zakrewsky, M., Gupta, V., Anselmo, A.C., Slee, D.H., Muraski, J.A., and Mitragotri, S. (2014). Topical delivery of siRNA into skin using SPACE-peptide carriers. *J. Control. Release* 179, 33–41.